

Coherent ρ^0 Production in Ultra-Peripheral Heavy Ion Collisions

C. Adler¹¹, Z. Ahammed²³, C. Allgower¹², J. Amonett¹⁴, B.D. Anderson¹⁴, M. Anderson⁵, G.S. Averichev⁹, J. Balewski¹², O. Barannikova^{9,23}, L.S. Barnby¹⁴, J. Baudot¹³, S. Bekele²⁰, V.V. Belaga⁹, R. Bellwied³¹, J. Berger¹¹, H. Bichsel³⁰, L.C. Bland², C.O. Blyth³, B.E. Bonner²⁴, A. Boucham²⁶, A. Brandin¹⁸, A. Bravar², R.V. Cadman¹, H. Caines²⁰, M. Calderón de la Barca Sánchez², A. Cardenas²³, J. Carroll¹⁵, J. Castillo²⁶, M. Castro³¹, D. Cebra⁵, P. Chaloupka²⁰, S. Chattopadhyay³¹, Y. Chen⁶, S.P. Chernenko⁹, M. Cherney⁸, A. Chikanian³³, B. Choi²⁸, W. Christie², J.P. Coffin¹³, T.M. Cormier³¹, J.G. Cramer³⁰, H.J. Crawford⁴, W.S. Deng², A.A. Derevschikov²², L. Didenko², T. Dietel¹¹, J.E. Draper⁵, V.B. Dunin⁹, J.C. Dunlop³³, V. Eckardt¹⁶, L.G. Efimov⁹, V. Emelianov¹⁸, J. Engelage⁴, G. Eppley²⁴, B. Erazmus²⁶, P. Fachini², V. Faine², K. Filimonov¹⁵, E. Finch³³, Y. Fisyak², D. Flierl¹¹, K.J. Foley², J. Fu^{15,32}, C.A. Gagliardi²⁷, N. Gagunashvili⁹, J. Gans³³, L. Gaudichet²⁶, M. Germain¹³, F. Geurts²⁴, V. Ghazikhanian⁶, O. Grachov³¹, V. Grigoriev¹⁸, M. Guedon¹³, E. Gushin¹⁸, T.J. Hallman², D. Hardtke¹⁵, J.W. Harris³³, T.W. Henry²⁷, S. Heppelmann²¹, T. Herston²³, B. Hippolyte¹³, A. Hirsch²³, E. Hjort¹⁵, G.W. Hoffmann²⁸, M. Horsley³³, H.Z. Huang⁶, T.J. Humanic²⁰, G. Igo⁶, A. Ishihara²⁸, Yu.I. Ivanshin¹⁰, P. Jacobs¹⁵, W.W. Jacobs¹², M. Janik²⁹, I. Johnson¹⁵, P.G. Jones³, E.G. Judd⁴, M. Kaneta¹⁵, M. Kaplan⁷, D. Keane¹⁴, J. Kiryluk⁶, A. Kisiel²⁹, J. Klay¹⁵, S.R. Klein¹⁵, A. Klyachko¹², A.S. Konstantinov²², M. Kopytine¹⁴, L. Kotchenda¹⁸, A.D. Kovalenko⁹, M. Kramer¹⁹, P. Kravtsov¹⁸, K. Krueger¹, C. Kuhn¹³, A.I. Kulikov⁹, G.J. Kunde³³, C.L. Kunz⁷, R.Kh. Kutuev¹⁰, A.A. Kuznetsov⁹, L. Lakehal-Ayat²⁶, M.A.C. Lamont³, J.M. Landgraf², S. Lange¹¹, C.P. Lansdell²⁸, B. Lasiuk³³, F. Laue², A. Lebedev², R. Lednický⁹, V.M. Leontiev²², M.J. LeVine², Q. Li³¹, S.J. Lindenbaum¹⁹, M.A. Lisa²⁰, F. Liu³², L. Liu³², Z. Liu³², Q.J. Liu³⁰, T. Ljubicic², W.J. Llope²⁴, G. LoCurto¹⁶, H. Long⁶, R.S. Longacre², M. Lopez-Noriega²⁰, W.A. Love², T. Ludlam², D. Lynn², J. Ma⁶, R. Majka³³, S. Margetis¹⁴, C. Markert³³, L. Martin²⁶, J. Marx¹⁵, H.S. Matis¹⁵, Yu.A. Matulenko²², T.S. McShane⁸, F. Meissner¹⁵, Yu. Melnick²², A. Meschanin²², M. Messer², M.L. Miller³³, Z. Milosevich⁷, N.G. Minaev²², J. Mitchell²⁴, V.A. Moiseenko¹⁰, C.F. Moore²⁸, V. Morozov¹⁵, M.M. de Moura³¹, M.G. Munhoz²⁵, J.M. Nelson³, P. Nevski², V.A. Nikitin¹⁰, L.V. Nogach²², B. Norman¹⁴, S.B. Nurushev²², J. Nystrand¹⁵, G. Odyniec¹⁵, A. Ogawa²¹, V. Okorokov¹⁸, M. Oldenburg¹⁶, D. Olson¹⁵, G. Paic²⁰, S.U. Pandey³¹, Y. Panebratsev⁹, S.Y. Panitkin², A.I. Pavlinov³¹, T. Pawlak²⁹, V. Perevoztchikov², W. Peryt²⁹, V.A. Petrov¹⁰, M. Planinic¹², J. Pluta²⁹, N. Porile²³, J. Porter², A.M. Poskanzer¹⁵, E. Potrebenikova⁹, D. Prindle³⁰, C. Pruneau³¹, J. Putschke¹⁶, G. Rai¹⁵, G. Rakness¹², O. Ravel²⁶, R.L. Ray²⁸, S.V. Razin^{9,12}, D. Reichhold⁸, J.G. Reid³⁰, F. Retiere¹⁵, A. Ridiger¹⁸, H.G. Ritter¹⁵, J.B. Roberts²⁴, O.V. Rogachevski⁹, J.L. Romero⁵, C. Roy²⁶, V. Rykov³¹, I. Sakrejda¹⁵, S. Salur³³, J. Sandweiss³³, A.C. Saulys², I. Savin¹⁰, J. Schambach²⁸, R.P. Scharenberg²³, N. Schmitz¹⁶, L.S. Schroeder¹⁵, A. Schüttauf¹⁶, K. Schweda¹⁵, J. Seger⁸, D. Seliverstov¹⁸, P. Seyboth¹⁶, E. Shahaliev⁹, K.E. Shestermanov²², S.S. Shimanskii⁹, V.S. Shvetsov¹⁰, G. Skoro⁹, N. Smirnov³³, R. Snellings¹⁵, P. Sorensen⁶, J. Sowinski¹², H.M. Spinka¹, B. Srivastava²³, E.J. Stephenson¹², R. Stock¹¹, A. Stolpovsky³¹, M. Strikhanov¹⁸, B. Stringfellow²³, C. Struck¹¹, A.A.P. Suaide³¹, E. Sugarbaker²⁰, C. Suire², M. Šumbera²⁰, B. Surrow², T.J.M. Symons¹⁵, A. Szanto de Toledo²⁵, P. Szarwas²⁹, A. Tai⁶, J. Takahashi²⁵, A.H. Tang¹⁴, J.H. Thomas¹⁵, M. Thompson³, V. Tikhomirov¹⁸, M. Tokarev⁹, M.B. Tonjes¹⁷, T.A. Trainor³⁰, S. Trentalange⁶, R.E. Tribble²⁷, V. Trofimov¹⁸, O. Tsai⁶, T. Ullrich², D.G. Underwood¹, G. Van Buren², A.M. VanderMolen¹⁷, I.M. Vasilevski¹⁰, A.N. Vasiliev²², S.E. Vigdor¹², S.A. Voloshin³¹, F. Wang²³, H. Ward²⁸, J.W. Watson¹⁴, R. Wells²⁰, G.D. Westfall¹⁷, C. Whitten Jr.⁶, H. Wieman¹⁵, R. Willson²⁰, S.W. Wissink¹², R. Witt³², J. Wood⁶, N. Xu¹⁵, Z. Xu², A.E. Yakutin²², E. Yamamoto¹⁵, J. Yang⁶, P. Yepes²⁴, V.I. Yurevich⁹, Y.V. Zanevski⁹, I. Zborovský⁹, H. Zhang³³, W.M. Zhang¹⁴, R. Zoukarneev¹⁰, A.N. Zubarev⁹

(STAR Collaboration)

¹Argonne National Laboratory, Argonne, Illinois 60439

²Brookhaven National Laboratory, Upton, New York 11973

³University of Birmingham, Birmingham, United Kingdom

⁴University of California, Berkeley, California 94720

⁵University of California, Davis, California 95616

⁶University of California, Los Angeles, California 90095

⁷Carnegie Mellon University, Pittsburgh, Pennsylvania 15213

⁸Creighton University, Omaha, Nebraska 68178

⁹Laboratory for High Energy (JINR), Dubna, Russia

¹⁰Particle Physics Laboratory (JINR), Dubna, Russia

¹¹University of Frankfurt, Frankfurt, Germany

- ¹²Indiana University, Bloomington, Indiana 47408
¹³Institut de Recherches Subatomiques, Strasbourg, France
¹⁴Kent State University, Kent, Ohio 44242
¹⁵Lawrence Berkeley National Laboratory, Berkeley, California 94720
¹⁶Max-Planck-Institut für Physik, Munich, Germany
¹⁷Michigan State University, East Lansing, Michigan 48824
¹⁸Moscow Engineering Physics Institute, Moscow Russia
¹⁹City College of New York, New York City, New York 10031
²⁰Ohio State University, Columbus, Ohio 43210
²¹Pennsylvania State University, University Park, Pennsylvania 16802
²²Institute of High Energy Physics, Protvino, Russia
²³Purdue University, West Lafayette, Indiana 47907
²⁴Rice University, Houston, Texas 77251
²⁵Universidade de Sao Paulo, Sao Paulo, Brazil
²⁶SUBATECH, Nantes, France
²⁷Texas A & M, College Station, Texas 77843
²⁸University of Texas, Austin, Texas 78712
²⁹Warsaw University of Technology, Warsaw, Poland
³⁰University of Washington, Seattle, Washington 98195
³¹Wayne State University, Detroit, Michigan 48201
³²Institute of Particle Physics, CCNU (HZNU), Wuhan, 430079 China
³³Yale University, New Haven, Connecticut 06520

The STAR collaboration reports the first observation of exclusive ρ^0 photo-production, $AuAu \rightarrow AuAu\rho^0$, and ρ^0 production accompanied by mutual nuclear Coulomb excitation, $AuAu \rightarrow Au^*Au^*\rho^0$, in ultra-peripheral heavy-ion collisions. The ρ^0 have low transverse momenta, consistent with coherent coupling to both nuclei. The cross sections at $\sqrt{s_{NN}} = 130$ GeV agree with theoretical predictions treating ρ^0 production and Coulomb excitation as independent processes.

PACS numbers: 25.20.-x, 25.75.DW, 13.60.-r

In ultra-peripheral heavy-ion collisions the two nuclei geometrically ‘miss’ each other and no hadronic nucleon-nucleon collisions occur. At impact parameters b significantly larger than twice the nuclear radius R_A , the nuclei interact by photon exchange and photon-photon or photon-Pomeron collisions [1]. Examples are nuclear Coulomb excitation, electron-positron pair and meson production, and vector meson production. The exchange bosons can couple coherently to the nuclei, yielding large cross sections. Coherence restricts the final states to low transverse momenta, a distinctive experimental signature. The STAR collaboration reports the first observation of coherent exclusive ρ^0 photo-production, $AuAu \rightarrow AuAu\rho^0$, and coherent ρ^0 production accompanied by mutual nuclear excitation, $AuAu \rightarrow Au^*Au^*\rho^0$, in ultra-peripheral heavy-ion collisions.

Exclusive ρ^0 meson production, $AuAu \rightarrow AuAu\rho^0$ (c.f. Fig. 1a), can be described by the Weizsäcker-Williams approach [2] to the photon flux and the vector meson dominance model [3]. A photon emitted by one nucleus fluctuates to a virtual quark-antiquark pair, which scatters elastically from the other nucleus and emerges as a vector meson. The gold nuclei are not disrupted, and the final state consists solely of the two nuclei and the vector meson decay products [4]. In the rest frame of the target nucleus, mid-rapidity ρ^0 production at RHIC

corresponds to a photon energy of 50 GeV and a photon-nucleon center-of-mass energy of 10 GeV. At this energy, Pomeron (\mathcal{P}) exchange dominates over meson exchange, as indicated by the rise of the ρ^0 production cross section with increasing energy in lepton-nucleon scattering [5].

In addition to coherent ρ^0 production, the exchange of virtual photons may excite the nuclei; these processes are believed to factorize for heavy-ion collisions. The process $AuAu \rightarrow Au^*Au^*\rho^0$ is shown in Fig. 1b. In lowest order, mutual nuclear excitation of heavy ions occurs by the exchange of two photons. Because of the Coulomb barrier for the emission of charged particles, nearly all nuclear decays following photon absorption include neutron emission [6].

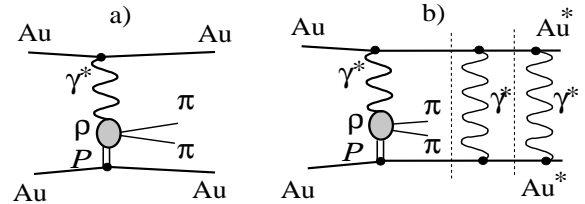


FIG. 1: Diagram for (a) exclusive ρ^0 production in ultra-peripheral heavy ion collisions, and (b) ρ^0 production with nuclear excitation. The dashed lines indicate factorization.

The photon and Pomeron can couple coherently to the gold nuclei. The wavelength $\lambda_{\gamma,P} > 2R_A$ leads to coherence conditions: a low transverse momentum of $p_T < \pi\hbar/R_A$ (~ 90 MeV/c for gold with $R_A \sim 7$ fm), and a maximum longitudinal momentum of $p_{\parallel} < \pi\hbar\gamma/R_A$ (~ 6 GeV/c at $\gamma = 70$), where γ is the Lorentz boost of the nucleus.

The ρ^0 production cross sections are large. The photon flux is proportional to the square of the nuclear charge Z^2 [2], and the cross section for elastic $\rho^0 A$ scattering scales as $A^{4/3}$ for surface coupling and A^2 in the bulk limit. At a center-of-mass energy of $\sqrt{s_{NN}} = 130$ GeV per nucleon-nucleon pair, a total ρ^0 cross section, regardless of nuclear excitation, $\sigma(AuAu \rightarrow Au^{(*)}Au^{(*)}\rho^0) = 350$ mb is predicted from a Glauber extrapolation of $\gamma p \rightarrow \rho^0 p$ data [4]. Calculations for coherent ρ^0 production with nuclear excitation assume that both processes are independent, sharing only a common impact parameter [4].

In the year 2000, the Relativistic Heavy Ion Collider (RHIC) at Brookhaven National Laboratory collided gold nuclei at $\sqrt{s_{NN}} = 130$ GeV. In the Solenoidal Tracker at RHIC (STAR) [7], charged particles are reconstructed with a 4.2 m long cylindrical time projection chamber (TPC) of 2 m radius [8]. The TPC operated in a 0.25 T solenoidal magnetic field. A central trigger barrel (CTB) of 240 scintillator slats surrounded the TPC. Two zero degree hadron calorimeters (ZDC) at ± 18 m from the interaction point were sensitive to the neutral remnants of nuclear break-up, with nearly 100% acceptance for neutrons from nuclear break-up through Coulomb excitation [9, 10].

Exclusive ρ^0 production has a distinctive signature: the $\pi^+\pi^-$ from the ρ^0 decay in an otherwise ‘empty’ detector. The tracks are approximately back-to-back in the transverse plane due to the small p_T of the pair. The gold nuclei remain undetected within the beam.

Two data sets are used in this analysis. For $AuAu \rightarrow AuAu\rho^0$, about 30,000 events were collected using a low-multiplicity ‘topology’ trigger. The CTB was divided in four azimuthal quadrants. Single hits were required in the opposite side quadrants; the top and bottom quadrants acted as vetoes to suppress cosmic rays. A fast on-line reconstruction [11] removed events without reconstructible tracks from the data stream. To study $AuAu \rightarrow Au^{(*)}Au^{(*)}\rho^0$, a data set of about 800,000 ‘minimum bias’ events, which required coincident detection of neutrons in both ZDCs as a trigger, is used.

Events are selected with exactly two oppositely charged tracks forming a common vertex within the interaction region. The ρ^0 candidates are accepted within a rapidity range $|y_\rho| < 1$. A systematic uncertainty of 5% is assigned to the number of ρ^0 candidates by varying the event selection criteria. The specific energy loss dE/dx in the TPC shows that the event sample is dominated by pion pairs. Without the ZDC requirement, cosmic rays are a major background. They are removed by requiring that the two pion tracks have an opening angle of less than 3 radians. Using the energy deposits in the ZDCs,

we select events with at least one neutron (xn,xn), exactly one neutron (1n,1n), or no neutrons (0n,0n) in each ZDC, and events with at least one neutron in exactly one ZDC (xn,0n); the latter two occur only in the topology trigger. A 10% uncertainty arises from the selection of single neutron signals.

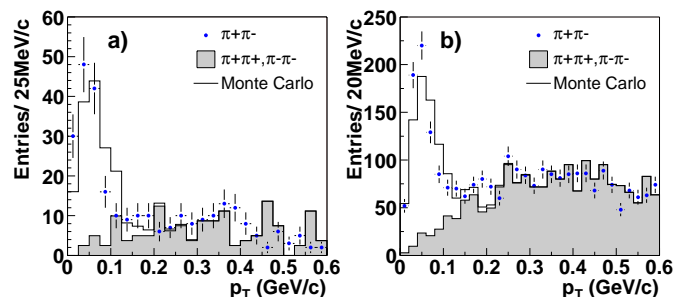


FIG. 2: The p_T spectra of pion pairs for the 2-track events selected by (a) the topology trigger (0n,0n) and (b) the minimum bias trigger (xn,xn). Points are oppositely charged pairs, and the shaded histograms are the normalized like-sign combinatorial background. The open histograms are simulated ρ^0 superimposed onto the background.

The transverse momentum spectra of pion pairs for the two-track event samples of the topology trigger (0n,0n) and the minimum bias trigger (xn,xn) are shown in Fig. 2. Both spectra are peaked at $p_T \sim 50$ MeV/c, as expected for coherent coupling. A background model from like-sign combination pairs, which is normalized to the signal at $p_T > 200$ MeV/c, is not peaked. For comparison, the p_T spectra from Monte Carlo simulations [4] are shown. They are normalized to the ρ^0 signal at $p_T < 150$ MeV/c and added to the background. The $M_{\pi\pi}$ invariant mass spectra (c.f. Fig. 4) for both event samples are peaked around the ρ^0 mass. We find 131 ± 14 (0n,0n) and 656 ± 36 (xn,xn) events at $p_T < 150$ MeV/c, which we define as coherent ρ^0 candidates. As $p_T \rightarrow 0$, the p_T spectra are expected to be altered by interference between the ρ^0 amplitudes from each nucleus [12], but the present statistics are insufficient to observe this effect. The simulations shown in Fig. 2 do not include interference.

The data contain combinatorial background contributions from grazing nuclear collisions and incoherent photon-nucleon interactions, which are statistically subtracted. Unrelated processes such as beam-gas and upstream interactions, cosmic rays, and pile-up events cause additional tracks not emerging from the primary vertex. These tracks are excluded by the vertex requirement. Incoherent ρ^0 production, where a photon interacts with a single nucleon, yields high p_T ρ^0 s, which are suppressed by the low pair p_T requirement; the remaining small contribution is indistinguishable from the coherent process. A coherently produced background arises from the misidentified two-photon process $AuAu \rightarrow Au^{(*)}Au^{(*)}e^+e^-$. It contributes mainly at low invariant mass $M_{\pi\pi} < 0.5$ GeV/c². Electrons with momenta $p < 140$ MeV/c can be identified by their energy loss dE/dx . About 30

e^+e^- pairs, peaked at low pair $p_T \sim 20$ MeV/c, were detected in the minimum bias data sample [13]. They are extrapolated to the full phase space using a Monte-Carlo simulation that describes e^+e^- pair production by lowest order perturbation theory [14]. Electron-positron pairs contribute $15 \pm 5\%$ to the signal at $p_T < 150$ MeV/c.

The acceptance and reconstruction efficiency were studied using a Monte Carlo event generator that reproduces the expected kinematic and angular distributions for ρ^0 production with and without nuclear excitation [4, 15], coupled with a detector simulation. These efficiencies are almost independent of p_T and the reconstructed invariant mass $M_{\pi\pi}$. For the minimum bias trigger, $41 \pm 5\%$ of all ρ^0 within $|y_\rho| < 1$ are reconstructed. The topology trigger vetoes the top and bottom of the TPC, reducing the geometrical acceptance. Pions with $p_T < 100$ MeV/c do not reach the CTB, effectively excluding pairs with $M_{\pi\pi} < 500$ MeV/c². Only $7 \pm 1\%$ of all ρ^0 with $|y_\rho| < 1$ are reconstructed in the topology trigger. The p_T resolution is 9 MeV/c. The $M_{\pi\pi}$ and rapidity resolutions are 11 MeV/c² and 0.01.

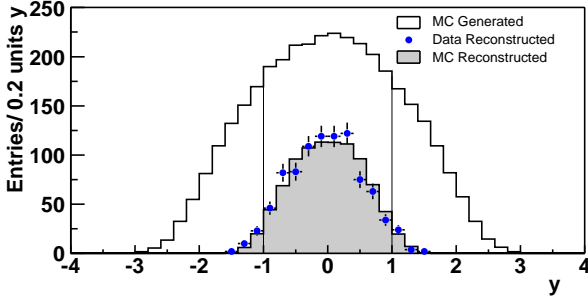


FIG. 3: Rapidity distribution of ρ^0 candidates (xn,xn) for the minimum bias data (points) compared to the normalized reconstructed (shaded histogram) and generated (open histogram) events from the Monte Carlo simulation.

The rapidity distribution for ρ^0 candidates (xn,xn) from the minimum bias data is shown in Fig. 3. It is well described by the reconstructed events from a simulation, which includes nuclear excitation [4]. The generated rapidity distribution is also shown. The acceptance is small for $|y_\rho| > 1$, so this region is excluded from the analysis. Cross sections are extrapolated from $|y_\rho| < 1$ to the full 4π acceptance by $\sigma_{4\pi}^\rho/\sigma_{|y_\rho|<1}^\rho = 1.7$ for ρ^0 production with nuclear break-up, and $\sigma_{4\pi}^\rho/\sigma_{|y_\rho|<1}^\rho = 2.2$ for ρ^0 production without nuclear break-up. A 15% uncertainty in the extrapolations is estimated by varying the Monte Carlo parameters.

The minimum bias data sample has an integrated luminosity of $L = 59$ mb⁻¹. The luminosity was measured by counting events containing more than 5 negatively charged hadrons with $p_T > 100$ MeV/c and pseudorapidity $|\eta| < 0.5$. These events represent 79% of the hadronic cross section [16]. We assume a total gold-gold hadronic cross section of 7.2 b [17]; its uncertainty dominates the 10% systematic uncertainty of L .

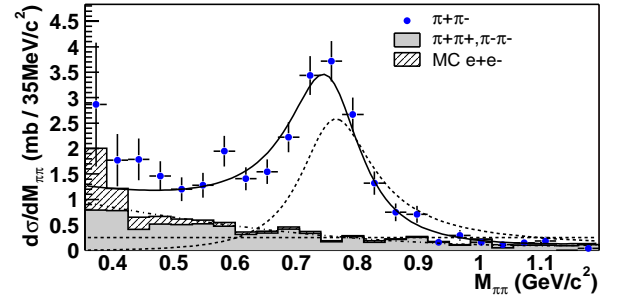


FIG. 4: The $d\sigma/dM_{\pi\pi}$ spectrum for 2-track (xn,xn) events with pair- $p_T < 150$ MeV/c in the minimum bias data. The shaded histogram is the combinatorial background, and the hatched histogram contains an additional contribution from coherent e^+e^- pairs. The fits are described in the text.

The $d\sigma/dM_{\pi\pi}$ invariant mass spectrum for the (xn,xn) events with a pair $p_T < 150$ MeV/c is shown in Fig. 4; the (0n,0n) events have a similar $d\sigma/dM_{\pi\pi}$ spectrum. The combinatorial background from normalized like-sign pairs and the contribution from coherent e^+e^- pairs are shown. The spectrum is fitted by the sum (solid) of a relativistic Breit-Wigner for ρ^0 production (dashed), a contribution from direct $\pi^+\pi^-$ production (dashed) and their interference (not shown) [3, 18, 19]:

$$\frac{d\sigma}{dM_{\pi\pi}} = \left| A \frac{\sqrt{M_{\pi\pi} M_\rho \Gamma_\rho}}{M_{\pi\pi}^2 - M_\rho^2 + i M_\rho \Gamma_\rho} + B \right|^2. \quad (1)$$

Here, Γ_ρ [19] is the momentum-dependent width including a phase space correction. A fixed polynomial contribution (dash-dotted) for the sum of combinatorial and coherent e^+e^- background is also included in the fit. The ρ^0 mass and width are consistent with accepted values [20]. The amplitude ratio for direct pion pair to ρ^0 production is $|B/A| = 0.81 \pm 0.07 \pm 0.20$ GeV^{-1/2}. The ratio $|B/A|$ is expected to decrease with increasing nuclear size due to increased pion absorption. However, our result is consistent with $|B/A| = 0.67 \pm 0.03$ GeV^{-1/2} found in $\gamma p \rightarrow \rho^0 p$ data [19].

For coherent ρ^0 production accompanied by mutual nuclear break-up (xn,xn), we measure a cross section of $\sigma(AuAu \rightarrow Au_{xn}^* Au_{xn}^* \rho^0) = 26.2 \pm 1.8 \pm 5.8$ mb in the two-track event sample, by extrapolating the integral of the Breit-Wigner fit to full rapidity. By selecting single neutron signals in both ZDCs, we obtain $\sigma_{1n,1n}^\rho/\sigma_{xn,xn}^\rho = 0.097 \pm 0.014$, so $\sigma(AuAu \rightarrow Au_{1n}^* Au_{1n}^* \rho^0) = 2.5 \pm 0.4 \pm 0.6$ mb. Single neutron emission is predominantly due to Coulomb excitation and the subsequent decay of the giant dipole resonance. The ratio $\sigma_{1n,1n}^\rho/\sigma_{xn,xn}^\rho$ agrees with $\sigma_{1n,1n}/\sigma_{xn,xn} = 0.12 \pm 0.01$ found for mutual Coulomb dissociation at RHIC [10], supporting that ρ^0 production and nuclear excitation are independent processes.

At $b \sim 2R_A$ coherent ρ^0 photo-production can overlap with grazing nuclear collisions, producing a low p_T ρ^0 accompanied by additional tracks. Additional tracks can

Cross Section	STAR (mb)	Ref [4] (mb)
$\sigma_{xn,xn}^\rho$	$26.2 \pm 1.8 \pm 5.8$	27
$\sigma_{1n,1n}^\rho$	$2.5 \pm 0.4 \pm 0.6$	3.25
$\sigma_{xn,xn}^{\rho(\text{inc.overlap})}$	$36.6 \pm 2.4 \pm 8.9$	—
$\sigma_{xn,0n}^\rho$	$90 \pm 55 \pm 20$	—
$\sigma_{0n,0n}^\rho$	$285 \pm 145 \pm 70$	—
σ_{total}^ρ	$410 \pm 190 \pm 100$	350

TABLE I: Comparison to predictions from [4]. The uncertainties are highly correlated.

also be produced at $b > 2R_A$ from nuclear excitation by high energy photons. At present, we can not differentiate between these two processes. The coherent (xn,xn) ρ^0 sample increases by 40% when events with additional tracks are included. Accounting for this, we find $\sigma^{\rho(\text{inc.overlap})}(AuAu \rightarrow Au_{xn}^* Au_{xn}^* \rho^0) = 36.6 \pm 2.4 \pm 8.9$ mb. For (1n,1n) events, no additional ρ^0 candidates are found with higher track multiplicities.

The major systematic uncertainties are in the 4π extrapolation (15%), acceptance and reconstruction efficiency (12%), luminosity determination (10%), and event selection (5%). The overlap region with grazing nuclear collisions contributes 10%; it does not contribute to $\sigma_{1n,1n}^\rho$, but a 10% uncertainty is due to the selection of the single neutrons. These contributions add in quadrature to 24% systematic uncertainty in the cross sections.

The absolute efficiency of the year 2000 topology trigger is poorly known and does not allow a direct cross section measurement. From the two-track events, we obtain the cross section ratios $\sigma_{xn,xn}^\rho/\sigma_{0n,0n}^\rho = 0.09 \pm 0.05$ and $\sigma_{xn,xn}^\rho/\sigma_{xn,0n}^\rho = 0.30 \pm 0.19$. The uncertainties reflect the small number of (xn,xn) and (xn,0n) events in the topology trigger data. Grazing nuclear collisions do not contribute to $\sigma_{0n,0n}^\rho$ and $\sigma_{xn,0n}^\rho$, since they yield neutron signals in both ZDCs. From $\sigma(AuAu \rightarrow Au_{xn}^* Au_{xn}^* \rho^0)$,

we estimate $\sigma(AuAu \rightarrow AuAu\rho^0) = 285 \pm 145 \pm 70$ mb, $\sigma(AuAu \rightarrow Au_{xn}^* Au\rho^0) = 90 \pm 55 \pm 20$ mb, and the total cross section for coherent ρ^0 production $\sigma(AuAu \rightarrow Au^{(*)}Au^{(*)}\rho^0) = 410 \pm 190 \pm 100$ mb.

Table I compares our results to the calculations of Ref. [4]. The calculation for $\sigma_{xn,xn}^\rho$ excludes grazing nuclear collisions; it is therefore compared to our value without the overlap correction. Recent predictions [21] are about 50% higher than in [4] without giving specific numbers for $\sqrt{s_{NN}} = 130$ GeV.

In summary, the first measurements of coherent ρ^0 production with and without accompanying nuclear excitation, $AuAu \rightarrow Au^*Au^*\rho^0$ and $AuAu \rightarrow AuAu\rho^0$, confirm the existence of vector meson production in ultra-peripheral heavy ion collisions. The ρ^0 are produced at small transverse momentum, showing the coherent coupling to both nuclei. The cross sections at $\sqrt{s_{NN}} = 130$ GeV are in agreement with theoretical calculations based on the Weizsäcker-Williams approach for large relativistic charges, the extrapolation from ρ^0 -nucleon to ρ^0 -nucleus scattering, and the assumption that ρ^0 production and nuclear excitation are independent processes.

We thank the RHIC Operations Group at Brookhaven National Laboratory for their tremendous support and for providing collisions for the experiment. This work was supported by the Division of Nuclear Physics and the Division of High Energy Physics of the Office of Science of the U.S. Department of Energy, the United States National Science Foundation, the Bundesministerium für Bildung und Forschung of Germany, the Institut National de la Physique Nucleaire et de la Physique des Particules of France, the United Kingdom Engineering and Physical Sciences Research Council, Fundacao de Amparo a Pesquisa do Estado de Sao Paulo, Brazil, and the Russian Ministry of Science and Technology.

-
- [1] G. Baur, K. Hencken and D. Trautmann, J. Phys. **G24**, 1657 (1998); C. A. Bertulani and G. Baur, Phys. Rep. **163**, 299 (1988).
 - [2] C. F. v. Weizsäcker, Z. Phys. **88**, 612 (1934); E.J. Williams, Phys. Rev. **45**, 729 (1934).
 - [3] J.J. Sakurai, Ann. Phys. **11** 1 (1960); T.H. Bauer *et al.*, Rev. Mod. Phys. **50** 261 (1978).
 - [4] S. R. Klein and J. Nystrand, Phys. Rev. C **60**, 014903 (1999); J. Nystrand, A. J. Baltz and S. R. Klein, *submitted to Phys. Rev. Lett.*, nucl-th/0205031 (2002). The cross sections for $\sqrt{s_{NN}} = 130$ GeV are a private communication.
 - [5] J.A. Crittenden, Springer Tracts in Modern Physics 140 (1997).
 - [6] B. L. Berman and S. C. Fultz, Rev. Mod. Phys. **47**, 713 (1975).
 - [7] K. H. Ackermann *et al.*, Nucl. Phys. **A661**, 681c (1999).
 - [8] H. Wieman *et al.*, IEEE Trans. Nucl. Sci. **44**, 671 (1997).
 - [9] C. Adler *et al.*, Nucl. Instrum. Methods **A470**, 488 (2001).
 - [10] M. Chiu *et al.*, nucl-ex/0109018 (2001).
 - [11] J. S. Lange *et al.*, Nucl. Instrum. Methods **A453**, 397 (2000).
 - [12] S. R. Klein and J. Nystrand, Phys. Rev. Lett. **84**, 2330 (2000).
 - [13] F. Meissner, nucl-ex/0112008 (2001).
 - [14] S. R. Klein and E. Scannapieco, STAR Note 243 (1996).
 - [15] J. Nystrand and S. R. Klein, nucl-ex/9811007 (1998).
 - [16] C. Adler *et al.*, Phys. Rev. Lett. **87**, 112303 (2001).
 - [17] A. J. Baltz, C. Chasman, and S. N. White, Nucl. Instrum. Methods **A417**, 1 (1998).
 - [18] P. Söding, Phys. Lett. **19**, 702 (1966).
 - [19] J. Breitweg *et al.*, Eur. Phys. J **C2**, 247 (1998).
 - [20] D. E. Groom *et al.*, Eur. Phys. J. **C15**, 1 (2000).
 - [21] L. Frankfurt, M. Strikman and M. Zhalov, hep-ph/0204175 (2002).